MEDICAL IMAGE SEGMENTATION FOR VIRTUAL ENDOSCOPY

László Szilágyi*, Zoltán Benyó*, Sándor M. Szilágyi**

**Department of Control Engineering and Information Technology*
Budapest University of Technology and Economics
Magyar tudósok krt. 2, 1117 Budapest, Hungary

***Faculty of Technical and Human Science*
Sapientia – Hungarian Science University of Transylvania
Marosvásárhely, Romania

Abstract: This paper presents new concepts in the design and implementation of a virtual endoscope. Starting from standard magnetic resonance images, and applying a two-step image processing, inner views of the human body can be obtained, even of such parts of the body, which cannot be penetrated by a traditional endoscope. The first step of the image processing consists in an enhanced version of the fuzzy C-means segmentation. Then a shape recovery algorithm is employed in order to reconstruct the 3-D object. The algorithms provide good-quality segmented images a very quick way, which makes them excellent tools to support a virtual endoscopy.

Keywords: image segmentation, fuzzy logic, image reconstruction, medical applications, computer tomography.

1. INTRODUCTION

Traditional endoscopes penetrate the human body in order to provide high resolution internal views of cavities and hollow organs. Even though such examinations are mostly considered non-invasive, the procedure causes pain, or at least discomforts the patient, who consequently needs some kind of sedation or anesthesia.

Magnetic resonance imaging (MRI) is a non-invasive diagnostic tool that views the internal anatomy of the human body in 2-D cross sections called slices. A virtual endoscope establishes 3-D internal views based on these sets of 2-D slices, using modern image processing techniques and computer graphics as well. Besides the comfort provided, another relevant advantage is the fact, that it can create images of any body part.

This paper presents a new concept of the virtual endoscope, being developed in the Biomedical Engineering Laboratory at TU Budapest. During the development process, MRI brain images are used for testing the methods, but the algorithm is capable to process other kinds of medical images, too. Consequently the virtual endoscope will have several medical applications.

In order to create a virtual endoscope based on magnetic resonance images, the following image processing tasks need to be performed (Fig. 1.):

1. Segmentation of the 2-D slices, to reduce the number of grey shades from 256 to 3, as required by medical scientists.

2. A shape recovery algorithm is applied to reconstruct the 3-D image of the brain.

3. Visualization via modern computer graphics tools.

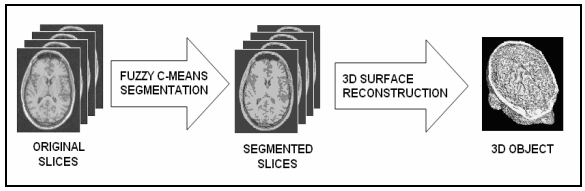

Fig. 1. Schematic representation of the whole image processing procedure

2. METHODS

2.1. 2-D Segmentation of medical images using an enhanced fuzzy C-means (FCM) algorithm

The standard FCM algorithm, introduced by Bezdek *et al.* (1991, 1993), groups the values x_k, $k = 1..n$ into c clusters, using the objective function

$$J_B = \sum_{i=1}^{c}\sum_{k=1}^{N} u_{ik}^{p}(x_k - v_i)^2 , \qquad (1)$$

where v_i represents the prototype value of the i th cluster, u_{ik} represents the fuzzy membership of the k th voxel with respect to cluster i, and p is a weighting exponent. By definition, for any k we have

$$\sum_{i=1}^{c} u_{ik} = 1 . \qquad (2)$$

To minimize the objective function, it is necessary to assign high membership values to those voxels, whose intensities are situated close to the prototype values of their particular clusters. FCM has several merits in brain image segmentation for its speed, but it performs no filtering, so the image quality remains poor.

In order to avoid this drawback, Ahmed *et al* (2002) proposed a modification to the original objective function by introducing a term that allows the labeling of a voxel to be influenced by the labels in its immediate neighborhood. This effect regularizes, and biases the solution toward piecewise-homogeneous labeling. It proved useful in segmenting images corrupted by salt and pepper noise. The modified objective function is given by

$$J_A = \sum_{i=1}^{c}\sum_{k=1}^{N}\left[u_{ik}^{p}(x_k - v_i)^2 + \frac{\alpha}{N_k}\sum_{r=1}^{N_k} u_{ik}^{p}(x_{k,r} - v_i)^2 \right], \qquad (3)$$

where $x_{k,r}$ represents the neighbor voxels of x_k, and N_k stands for the number of voxels in the neighborhood of the k th voxel. The parameter α controls the intensity of the neighboring effect. These modifications led to better image quality, but the performance in time is very slow.

In the followings, some modifications will be introduced to these algorithms. MR brain images are stacks of approximately 200 slices, which at their turn represent large matrices of voxels. A set of MR brain image slices contains around ten million (10^7) voxels. The intensity of the voxels is generally encoded with 8 bit resolution, that is, there are only 256 possible levels of intensity for each voxel. To considerably reduce the amount of calculations performed during the segmentation process, the algorithm will be modified the following way.

Step 1. First we apply a local filtering to each voxel. Let us consider the neighborhood of the k th voxel, as described by Ahmed *et al.* (2002). Let us denote by ξ_k the filtered intensity level of the k th voxel, and we will compute it as follows:

$$\xi_k = \frac{1}{1+\alpha}\cdot\left(x_k + \frac{\alpha}{N_k}\sum_{r=1}^{N_k} x_{k,r} \right). \qquad (4)$$

Voxel intensity levels have normalized values, they are situated in the [0,1] interval.

Step 2. Let us denote the number of intensity levels by q. As it was previously stated, q is much smaller then N. We denote by γ_l the number of pixels from the whole stack of slices, having the intensity equal to l, where $l = 1..q$, Szilágyi et al (2003). By definition, the following equality holds:

$$\sum_{l=1}^{q} \gamma_l = N . \qquad (5)$$

Step 3. The objective function used for the segmentation of the filtered signal will be:

$$J_S = \sum_{i=1}^{c}\sum_{l=1}^{q} \gamma_l u_{il}^{p}(\xi_l - v_i)^2 . \qquad (6)$$

We need to find those values of the parameters u_{il} and v_i, for which this objective function has the minimum value. Let us consider the Lagrange multiplier defined according to the following formula:

$$F_S = \sum_{i=1}^{c}\sum_{l=1}^{q}\left[\gamma_l u_{il}^{p}(\xi_l - v_i)^2\right] + \sum_{l=1}^{q}\lambda_l\left(1 - \sum_{i=1}^{c} u_{il}\right). \qquad (5)$$

Step 4. Taking the derivative of F_S with respect to u_{il}, and equaling it to 0, we get:

$$\frac{\delta F_S}{\delta u_{il}} = p\gamma_l u_{il}^{p-1}(\xi_l - v_i)^2 - \lambda_l = 0 , \qquad (6)$$

and consequently

$$u_{il} = \left(\frac{\lambda_l}{p\gamma_l}\right)^{\frac{1}{p-1}} (\xi_l - v_i)^{\frac{-2}{p-1}} . \qquad (7)$$

Applying (2), we obtain

$$\lambda_l = p\gamma_l\left[\sum_{j=1}^{c}(\xi_l - v_j)^{\frac{-2}{p-1}}\right]^{1-p} , \qquad (8)$$

and so

$$u_{il} = \left[\sum_{j=1}^{c} \left(\frac{\xi_l - v_i}{\xi_l - v_j} \right)^{\frac{2}{p-1}} \right]^{-1} . \qquad (9)$$

Step 5. Taking the derivative of F_S with respect to v_i, and equaling it to 0, we get:

$$\frac{\delta F_S}{\delta v_i} = -2 \cdot \sum_{l=1}^{q} \left(\gamma_l u_{il}^p (\xi_l - v_i) \right) = 0 , \qquad (10)$$

and consequently

$$v_i = \left(\sum_{l=1}^{q} \gamma_l u_{il}^p \xi_l \right) \left(\sum_{l=1}^{q} \gamma_l u_{il}^p \right)^{-1} . \qquad (11)$$

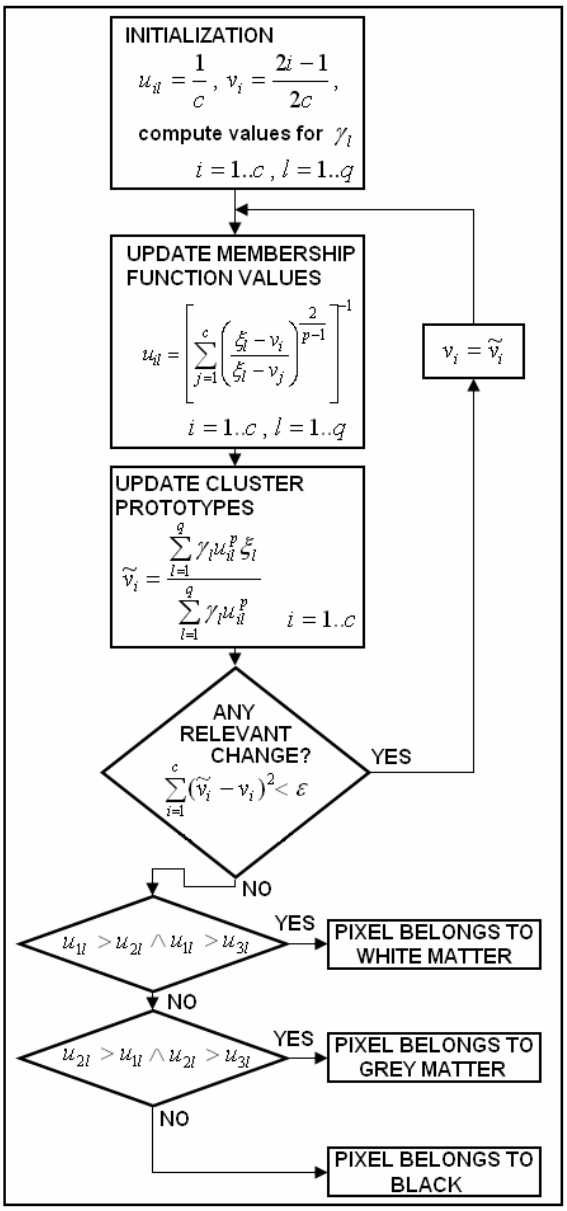

Fig. 2. The algorithm of the 2-D segmentation

The enhanced FCM algorithm for MR brain image segmentation can be summarized as follows:

a. Determine the values of $\{\gamma_l\}_{l=1}^{q}$, select initial cluster prototypes $\{v_i = (2i-1)/(2c)\}_{i=1}^{c}$.

b. Update membership function values according to (9).

c. Compute the new values for cluster prototypes according to (11).

d. Repeat b-c until the Euclidean norm of the change of the prototype vector is smaller then a previously set small positive number ε.

2.2. Reconstruction of the 3-D object from the segmented slices

The shape recovery or reconstruction of the 3-D object is performed according to the following idea:

Starting from the segmented slices obtained using the FCM algorithm, three scalar spaces are defined, corresponding to the black matter, grey matter and white matter, according to this formula: $R_{ik} = 1 - 2u_{ik}$. The value povided so is negative if the pixel k is inside the region i, positive if it is outside, and is zero at the surface of the region i.

Then a parametrized small closed surface is defined inside the region whose boundaries are wished to be detected. In order to lead this closed surface to the boundary of the region, such an objective function is needed, which contains the square of all R_{ik} values.

Several solutions exists to this problem, some remarkable ones are presented by Fan *et al* (2002), van Ginneken *et al* (2002), Marroquin *et al* (2002), Pitiot *et al* (2002), Suri *et al* (2002b), and Wink *et al* (2002), while Suri *et al* (2002a) gives a great comparison of such methods.

The first 3-D reconstructed surfaces presented in this paper have been obtained using a generalized marching cube algorithm. Elastic surface driven solutions are still under construction.

3. RESULTS

Medical requirements at brain imaging generally use segmentation into three clusters, corresponding to background, gray matter, and white matter. Fig. 3 presents a brain MRI example, an original image with 256 grey levels, and a segmented version of the same slice, obtained using the enhanced FCM method.

The cluster prototype grey levels show a quick convergence, which is illustrated in Fig. 4. Practically after 2 or 3 cycles they do not change.

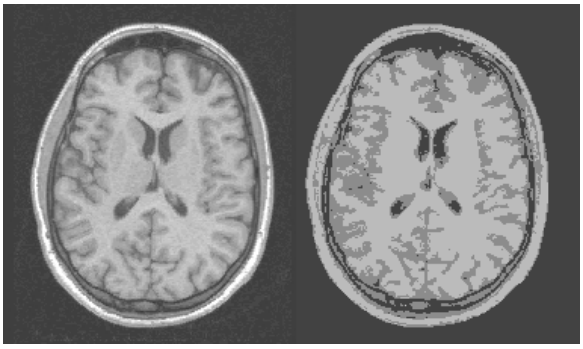

Fig. 3. Original MR brain cross section (left), and segmented brain slice (right)

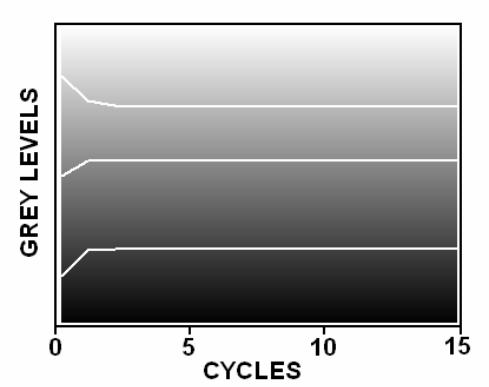

Fig. 4. Convergence of cluster prototypes in case of three clusters

The parameters introduced in the previous section, namely p, α, and N_k largely influence the efficiency of the algorithm. For example, if the exponent p is smaller than 1, the algorithm will not converge at all. BCFCM algorithm uses $p = 2$, which slightly simplifies the calculations, but this value does not assure the quickest convergence. Fig. 5 shows the relation between the objective functions J_A (with $p = 2$) and J_S (with $p = 1.2$), and makes it visible, that after two or more cycles we get $\left|J_A - J_{A_{\min}}\right| \Big/ \left|J_S - J_{S_{\min}}\right| \approx 5$, which means the proposed algorithm needs less cycles to get the same accuracy.

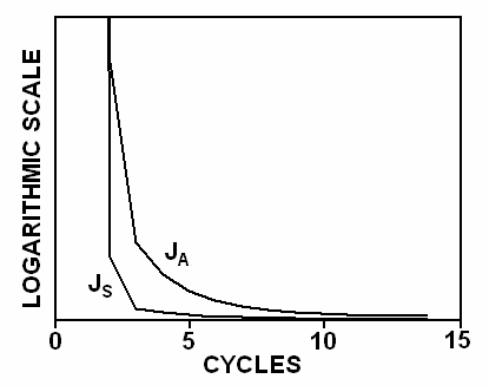

Fig. 5. Convergence of the objective function

The quality of filtering depends on the chosen neighborhood effect, and its intensity value α. This α has to be great enough so that it eliminates most of the salt and pepper noise, but it also has to be small enough, so that the image will not lose much of its sharpness. The optimal value of α varies between 0.5 and 1.2. The cardinality of the neighborhood taken in consideration for each pixel also influences the quality of the obtained image. A necessary and sufficient choice is to use a neighborhood, which contains the 8 immediate neighbors of the pixel.

Because of the considerable difference between the number of pixels in an MR slice (or the whole brain volume) (N), and the number of grey intensity levels of the original image (q), the amount of calculation, that is needed to perform during each cycle, is reduced by the new method approximately 40 times.

Fig. 6 shows some of the first 3-D images obtained using the described methods. Results are promising, but in order to visualize smaller details of the human body with the right accuracy, MR images with higher resolution will be needed.

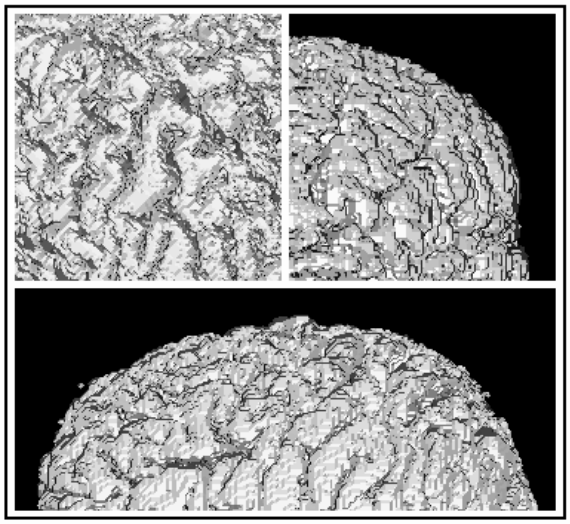

Fig. 6. Some brain images obtained using the described methods

4. CONCLUSION

The proposed algorithm provides a slight improvement in the quality of segmented brain images, and it performs significantly quicker then its ancestors. The smooth boundaries between the black, grey, and white matter, shown in Fig. 3, will lead to good quality 3-D images. These make the algorithms capable to support a virtual brain endoscope.

ACKNOWLEDGMENT

This research was supported by the Hungarian National Research Fund (OTKA), Grants No.

T042990, T029830, and U047793, Sapientia KPI, and the Pro Progressio Foundation.

REFERENCES

Ahmed M.N., S.M. Yamany, N. Mohamed, A.A. Farag, T. Moriarty (2002), A Modified Fuzzy C-Means Algorithm for Bias Field Estimation and Segmentation of MRI Data, *IEEE Transactions on Medical Imaging*, **21**, No. 3, pp. 193-199.

Bezdek, J.C., S.K. Pal (1991), *Fuzzy Models for Pattern Recognition, Piscataway*, NJ: IEEE Press.

Bezdek, J.C., L. Hall, L. Clarke (1993), Review of MR image segmentation using pattern recognition, *Med. Phys.*, **20**, pp. 1033-1048.

Fan Y., T. Jiang, D.J. Evans (2002), Volumetric Segmentation of Brain Images Using Parallel Genetic Algorithms, *IEEE Transactions on Medical Imaging,* Vol. 21., No. 8, pp. 904-909.

van Ginneken, B., A.F. Frangi, J.J. Staal, B.M. ter Haar Romeny, M.A. Viergever (2002), Active Shape Model Segmentation With Optimal Features, *IEEE Transactions on Medical Imaging,* **21**., No. 8, pp. 924-933.

Marroquin J.L., B.C. Vemuri, S. Botello, F. Calderon, A. Fernandez-Bouzas (2002), An Accurate and Efficient Bayesian Method for Automatic Segmentation of Brain MRI, *IEEE Transactions on Medical Imaging,* **21**., No. 8, pp. 934-945.

Pitiot, A., A.W. Toga, P.M. Thompson (2002), Adaptive Elastic Segmentation of Brain MRI via Shape-Model-Guided Evolutionary Programming, *IEEE Transactions on Medical Imaging,* **21**., No. 8, pp. 910-923.

Suri J.S., K. Liu, S. Singh, S. Laxminarayan, X. Zeng, L. Reden (2002a), Shape Recovery Algorithms Using Level Sets in 2-D/3-D Medical Imagery: A State-of-the-Art Review, *IEEE Transactions on Information Technology in Biomedicine,* **6**., No. 1., pp. 8-28.

Suri J.S., K. Liu, L. Reden, S. Laxminarayan (2002b), A review on MR vascular image processing: skeleton versus nonskeleton approaches, *IEEE Transactions on Information Technology in Biomedicine,* **6**., No. 4., pp. 338-350.

Szilágyi L., Z. Benyó, S. M. Szilágyi, H. S. Adam (2003), MR Brain Image Segmentation Using an Enhanced Fuzzy C-Means Algorithm, *Proceedings of the 25th International Conference of IEEE/EMBS*, Cancún, Mexico, **1**, pp. 724-726.

Wink O., W.J. Niessen, M.A. Viergever (2000), Fast Delineation and Visualization of Vessels in 3-D Angiographic Images, *IEEE Transactions on Medical Imaging,* Vol. 19., No. 4, pp. 337-346.